  Bull. Chem. Soc. Jpn., 57, 2703—2711 (1984)

Reversing-Pulse Electric Birefringence of Poly(γ-methyl L-glutamate) in Hexafluoro-2-propanol

Kazuyoshi UEDA

Faculty of Science, Hiroshima University, Higashisenda-machi, Naka-ku, Hiroshima 730

(Received March 8, 1984)

Reversing-pulse electric birefringence (RPEB) signals of poly(γ-methyl L-glutamate) (PMLG) were measured, for the first time, in hexafluoro-2-propanol at 25 °C and at 535 nm. Quantitative analyses were carried out on the steady-state birefringence and the field-free decay time ($<\tau>_{EB}$) in the wide field strength region and also on the rise, reverse, and decay portions in the low field strength region by taking into account the continuous molecular length distribution of a fractionated PMLG sample. The weight-average length (l_w), permanent dipole moment (μ_w), polarizability anisotropy ($\Delta\alpha_w$), and the degree of polydispersity (l_w/l_n) were evaluated by two procedures: one from the analysis of the reverse-transient portion and the other from the field-free decay portion of RPEB signals. These two sets of the parameters should be identical with each other, if the electrooptical and hydrodynamic properties of PMLG do not change during the field-on and field-off processes. However, the length of the PMLG helix is shorter by about 18% in the presence of an electric field than that in the absence of the field. In order to explain this discrepancy, a new concept of reversible conformational transition under the external electric field is introduced.

Poly(γ-methyl L-glutamate) (PMLG) in solution has been studied by the methods of spectroscopy, circular dichroism, linear dichroism,[1-3] in order to resolve an important optical problem, that is, the strong-coupling exciton theory of the helical polypeptide.[4-6] For this purpose the PMLG molecule has been regarded as a suitable model, because it has no strongly absorbing chromophore in the side chain in the far ultraviolet region and exists as a helix in some organic solvents. In order to clarify the optical properties, the exact solution conformation of PMLG must be confirmed. However, few reports have appeared on this subject.[7,8] Although the electric birefringence (EB) is very useful for such studies,[9-11] only one study was reported, in which the Kerr constant of PMLG was measured in a mixed organic solvent.[7]

In this work, the reversing-pulse electric birefringence (RPEB) of PMLG in hexafluoro-2-propanol (HF2P) has been measured to determine the hydrodynamic and electrooptical properties in detail. Recently, some analytical procedures have been developed for the experimental data of polydisperse systems which were obtained by the rectangular pulse EB[12-16] and electric dichroism[17] methods. These enable one to estimate the weight-average molecular length and the breadth of the distribution from the decay signals. As compared with those methods, the RPEB method has a special feature that the parameters, which characterize the molecular weight distribution, can be determined independently from the two portions of a transient signal; one from the field-free decay and the other from the field-on reverse portion.[18,19] Therefore, the two sets of the molecular parameters obtained respectively in the presence and the absence of an external electric field may be compared. The results indicate that the transient processes in these two portions differ from each other.

The purposes of this work are (1) to evaluate quantitatively the discrepancy between the reverse and the decay processes involved in the RPEB signals of PMLG in HF2P by taking into account the molecular length distribution, (2) to clarify the electrooptical properties and solution conformation, and (3) to ascertain the effect of the applied electric field. The results are discussed by assuming some possible causes, such as molecular association, flexibility, partial destruction of helix, and electric field-induced conformational transition. By simulating the rise, reverse, and decay processes of the RPEB signal, a possible conformational change under the electric field is proposed on the basis of the change of the molecular length of the PMLG helix.

Experimental

Materials and Viscometric Characterization. Poly(γ-methyl L-glutamate), (PMLG), was purchased from Pilot Chemicals, Inc. (Watertown, Mass., USA). It was prepared by polymerizing the corresponding *N*-carboxyanhydride with sodium methoxide in dioxane. The specific viscosity, η_{sp}/c, [c=0.2% in dichloroacetic acid (DCA)] was 3.40, as supplied by the manufacturer. This sample was dissolved in chloroform and the solution was filtered to remove insoluble lumps. The PMLG sample in the clear solution was fractionated into five fractions with ethanol as precipitant by the successive precipitation method.[11] The third fraction was used in the present work. 1,1,1,3,3,3-Hexafluoro-2-propanol (HF2P) for spectroscopy (Merck) was used without further purification. Reagent-grade DCA (Tokyo Kasei Kogyo Co.) was shaken with P_2O_5 and then kept overnight in the dark. The supernatant was distilled under reduced pressure at 6 mmHg (1 mmHg=133.3 Pa) in a nitrogen gas atmosphere.[20] PMLG was dissolved in HF2P and in DCA after drying under reduced pressure at 78.3 °C for 10 h. The viscosity of all samples was measured in a Ubbelohde-type dilution viscometer at 25 °C. The intrinsic viscosity of PMLG in DCA, $[\eta]_{DCA}$, was 267 cm³/g in the concentration range 1.0—11.0 mM (1 mM=10^{-3} mol dm^{-3}). The concentration of PMLG was expressed in terms of monomer units throughout this work. From the value of $[\eta]_{DCA}$, the weight-average molecular weight (M_w) was estimated to be 13.5×10^4 (the degree of polymerization, DP_w, is 943) by using the relationship between $[\eta]_{DCA}$ and M_w which was obtained by Okamoto and Sakamoto.[7] The intrinsic viscosity of PMLG in HF2P, $[\eta]_{HF2P}$, was found to be 931 cm³/g in the concentration range 1.7—10.6 mM). The viscosity of HF2P was also obtained to be 1.595 cP (1 cP=10^{-3} Pa s).

RPEB Measurements. All RPEB signals were measured at 25 °C and at 535 nm on an apparatus which was designed

and constructed in this laboratory.[18,21] The data acquisition and processing were achieved with a system consisting of a two channel transient wave memory (Riken Denshi Model TCH-4000(s), whose maximum sampling time is 50 ns/word, 8 bit, 4 kw) and of a microcomputer (Oki Denki IF-800 Model 10).[22] The signals were accumulated in arbitrary numbers, averaged, and then stored on a floppy disk. A quarter-wave plate was inserted in the optical path. The electric birefringence, Δn, was expressed as $\Delta n=\lambda\delta/2\pi d$, where δ is the phase retardation, λ is the wavelength *in vacuo*, and d is the optical path length of a Kerr cell, which was made of Kel-F.[23] The electrode gaps are 0.207 cm (d=1.0 cm) and 0.33 cm (d=2.0 cm), respectively. The Kerr constant of HF2P, B_{HF2P}, was found to be positive and 5.6×10^{-13} cm V^{-2}. This value is very small compared with the Kerr constant of PMLG solution, but cannot be ignored for a dilute PMLG solution ($c\leq0.49$ mM); hence, the phase retardation, δ_{HF2P} ($=2\pi dBE^2$), was subtracted from the δ values observed for dilute solutions.

Analysis of Data. For a polydisperse polymer solution, in which rigid rodlike solutes show a continuous distribution of molecular weights, *i. e.*, lengths, the steady-state electric birefringence at an arbitrary electric field strength E is expressed with the weight-average orientation function, $\langle\Phi\rangle_w$, as[15,24]

$$\Delta n(\infty)=\frac{2\pi\bar{C}_v}{n}(g_3-g_1)\langle\Phi(\beta(l),\gamma(l))\rangle_w, \tag{1}$$

where n is the refractive index of the solution, $\bar{C}_v$ is the volume fraction of the solute, and (g_3-g_1) is the optical anisotropy factor. $\beta(l)=\mu(l)E/kT$ and $\gamma(l)=\Delta\alpha(l)E^2/kT$, where $\mu(l)$ is the permanent dipole moment and $\Delta\alpha(l)$ is the polarizability anisotropy of the molecule with length l.

In the low electric field region where the Kerr law holds, the reverse portion of a normalized RPEB signal is expressed as[18,25]

$$\frac{\Delta n(t)}{\Delta n(\infty)}=\frac{\int_a^b\Delta n(\infty,l)\left\{1-\frac{3\beta(l)^2}{\beta(l)^2+2\gamma(l)}(e^{-2\theta_{11}(l)t}-e^{-6\theta_{11}(l)t})\right\}dl}{\int_a^b\Delta n(\infty,l)dl}, \tag{2}$$

where θ_{11} is the rotary diffusion coefficient of the cylindrical molecule with a diameter of $2b$. In this work, θ_{11} is calculated by using Broersma's equation.[26] $\Delta n(\infty,l)=(2\pi\bar{C}_v/15n)\times(g_3-g_1)\,\phi(l)\,[\beta(l)^2+2\gamma(l)]$, where $\phi(l)$ is the fraction of solute molecules with length l. $\phi(l)$ is proportional to $lf_n(l)$, where $f_n(l)$ is the probability density function, which is defined on the basis of the number of solute molecules.[13,15] The length distribution of PMLG molecules in a soluion is assumed to be logarithmic-normal (the Lansing-Kraemer distribution).[27] Then, $f_n(l)$ was given by[28]

$$f_n(l)=\frac{1}{\omega l\sqrt{\pi}}\exp\left[-\frac{1}{\omega^2}\left(\ln\frac{l}{l_L}\right)^2\right], \tag{3}$$

where ω and l_L are parameters with which the weight-average molecular length, l_w, may be defined as $l_w=l_L(l_w/l_n)^{3/2}$ and the degree of polydispersity, expressed in terms of the ratio of weight- to number-average lengths, l_w/l_n, as $l_w/l_n=\exp(\omega^2/2)$. Similarly, the rise portion of the same RPEB signal is given as[29]

$$\frac{\Delta n(t)}{\Delta n(\infty)}=1-\frac{\int_a^b\Delta n(\infty,l)\left\{\frac{3\beta(l)^2e^{-2\theta_{11}(l)t}-[\beta(l)^2-4\gamma(l)]e^{-6\theta_{11}(l)t}}{2[\beta(l)^2+2\gamma(l)]}\right\}dl}{\int_a^b\Delta n(\infty,l)dl}. \tag{4}$$

The decay portion is written as

$$\frac{\Delta n(t)}{\Delta n(0)}=\frac{\int_a^b\Delta n(0,l)e^{-6\theta_{11}(l)t}dl}{\int_a^b\Delta n(0,l)dl}, \tag{5}$$

where $\Delta n(0,l)\equiv\Delta n(\infty,l)$. In all calculations, the upper and lower integral limits a and b were set as 50 and 6450 Å instead of (0, ∞).

The intrinsic viscosity for thin rods can also be calculated by taking into account the polydispersity of molecular lengths. By using Simha's equation,[30] it can be expressed as follows:

$$\frac{\langle[\eta]\rangle}{\bar{v}}=\frac{\int_a^b lf_n(l)\left\{\left(\frac{l}{2b}\right)^2\left[\frac{1}{15(\ln l-\ln b-1.8)}+\frac{1}{5(\ln l-\ln b-0.8)}\right]+\frac{14}{15}\right\}dl}{\int_a^b lf_n(l)dl}, \tag{6}$$

where $\bar{v}$ is the average partial specific volume of solutes and $\langle[\eta]\rangle$ is the weight-average intrinsic viscosity.[29,31] Once the $f_n(l)$ is determined from Eq. 3 with the parameters l_w and l_w/l_n which are obtained from the reverse-transient analysis by assuming an appropriate value of b, $\langle[\eta]\rangle$ can be calculated from Eq. 6. By comparing the calculated $\langle[\eta]\rangle$ with the experimentally obtained $[\eta]$, the selection can be made for the most probable value of b that reproduces both the observed $[\eta]$ and the reverse-transient signal from several likely values of b by an iteration procedure.[29]

Results and Discussion

Steady-state Birefringence of PMLG. Figure 1 shows a typical RPEB signal of PMLG in HF2P with an applied pulse field. In this case, twenty signals were accumulated and then averaged to improve the signal-to-noise ratio. After an electric pulse is applied, the signal rises, reaches a steady-state, then decays to the baseline after the pulse is terminated. The sign of the signal is positive. Similarly to the previous cases of poly(α-L-glutamic acid), (PGA),[18] and poly(γ-benzyl L-glutamate), (PBLG),[29] the RPEB signal of PMLG

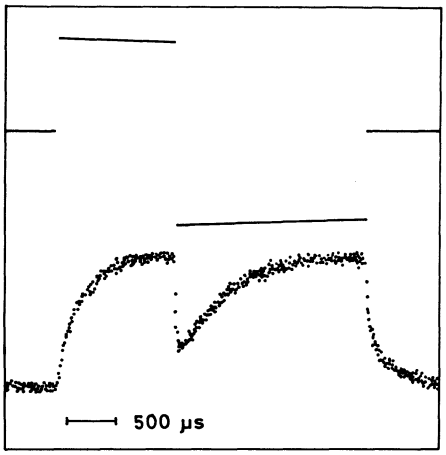

Fig. 1. A typical RPEB signal of PMLG in HF2P and an applied electric pulse field. The signal was digitized with a transient wave memory and averaged twenty-fold in real time with a microcomputer. The sampling time is 1 μs/word. The concentration: 7.82 mM. The field strength: 3.39 kV/cm.

shows a large dip in the reverse portion. This result immediately indicates that the permanent dipole moment contributes to the electric field orientation of PMLG.[25] Figure 2 shows the dependence of the steady-state phase retardation δ on field strength. Values of δ tend to saturate at higher fields, but are proportional to the square of field strength in the low field region ($E<3.5$ kV/cm), that is, the Kerr law holds (insert).

The Kerr constant, B, is defined as

$$B = \frac{1}{\lambda}\left[\frac{\Delta n}{E^2}\right]_{E\to 0} = \frac{1}{2\pi d}\left[\frac{\delta}{E^2}\right]_{E\to 0}. \quad (7)$$

Figure 3 shows plots of δ/E^2 against the square of electric field strength. Values of δ/E^2 are nearly constant below 3.5 kV/cm. By extrapolating these values to zero field strength, the Kerr constant was calculated. The specific Kerr constant, B/c, is given in Table 1, and also shown in Fig. 4(a). The values of B/c are independent of the concentration of PMLG. The intrinsic Kerr constant, $(B/c)_{c\to 0}$, was found to be 6.2×10^{-7} cm^4 g^{-1} V^{-2}. This value is rather small: about one half of the intrinsic Kerr constant obtained for PBLG[19] and about one-third for PGA[18] of almost the same molecular size.

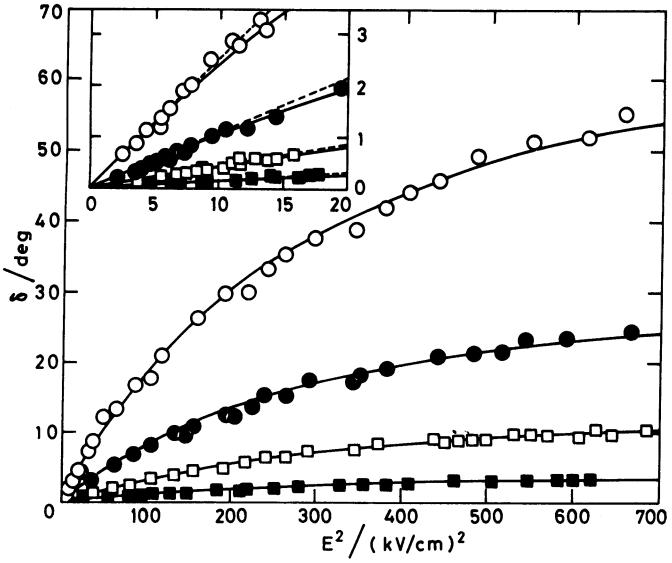

Fig. 2. The field-strength dependence of the steady-state electric birefringence, δ, of PMLG in HF2P. Insert: the low field strength region. The concentrations of PMLG are 7.82 mM (○), 3.52 mM (●), 1.41 mM (□), and 0.49 mM (■). The solid lines represent the theoretical curves with parameters in Table 2. The dotted lines represent the Kerr law.

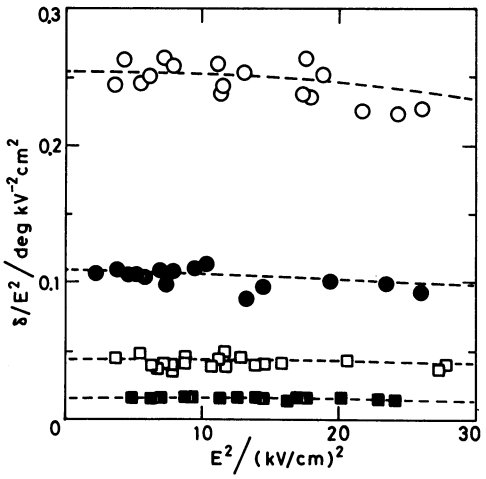

Fig. 3. The phase retardation per square of field strength, δ/E^2, in the low field strength region. Symbols are the same as in Fig. 2.

In order to investigate the aggregation of PMLG helices, values of δ at four electric field strengths were measured in detail over a wide range of concentrations. For example, the values of δ/c were still almost constant at a fifty-fold dilution (0.15 mM), as plotted in Fig. 4(b). Since they would change with molecular association,[32-34] no intermolecular association of PMLG seems to occur below 8 mM. This conclusion is also confirmed in the later section, where the relation between the molecular weight and molecular length is discussed.

Reverse-transient Process of PMLG. The minimum in the reverse portion of an RPEB signal can be specified by t_m, the time required for the signal to reach the minimum after the pulse reversal, and Δ_m, the height from the baseline at t_m. Both t_m and Δ_m are

Table 1. Specific Kerr constant B/c, reverse-transient minimum position, $(t_m)_{E\to 0}$ and $(\Delta_m)_{E\to 0}$, and weight-average relaxation time, $\langle\tau\rangle_w$, of PMLG in HF2P at various concentrations c.

c	B/c	$(t_m)_{E\to 0}$	$(\Delta_m)_{E\to 0}$	$\langle\tau\rangle_w$
mM	10^{-7}cm^{4}g^{-1}V^{-2}	μs		μs
7.82	6.3	80.0	0.33	94.5
3.52	6.1	69.0	0.38	81.0
1.41	6.2	64.5	0.38	70.0
0.49	6.4	56.0	0.36	63.0

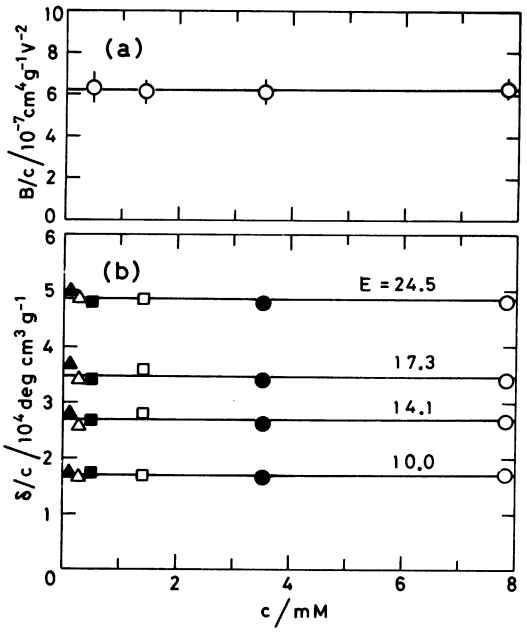

Fig. 4. (a) The dependence of the specific Kerr constant, B/c, on concentration and (b) the dependence of δ/c on concentration at four selected field strengths. The field strength, E, in kV/cm. In (b) the symbols are the same as in Fig. 2; moreover, two lower concentrations, 0.3 mM (△), 0.15 mM (▲), are also added.

plotted against the square of field strength in Fig. 5. The limiting values at zero field strength, $(t_m)_{E\to 0}$ and $(\Delta_m)_{E\to 0}$, are given in Table 1. From these values, the reverse portion of the RPEB signal can be analyzed with the aid of Eq. 2 to determine the values of l_w, l_w/l_n, and $(\beta_w)^2/2\gamma_w$. (This procedure was shown in detail in Figs. 7 and 8 in Ref. 18.) The theoretical orientation function $\langle\Phi\rangle_w$ can then be calculated with those parameters [l_w, l_w/l_n, $(\beta_w)^2/2\gamma_w$] which are given in Table 2. By comparing $\langle\Phi\rangle_w$ with experimentally obtained δ values in a wide range of field strengths, on a double logarithmic plot, the values of μ_w, $\Delta\alpha_w$, and the optical anisotropy factor (g_3-g_1) can be obtained separately (the matching procedure).[11,35] These values are also given in Table 2. The best-fitted theoretical curve of δ was calculated by using these values with the aid of Eq. 1, and is shown in Fig. 2 by a solid line at each concentration of PMLG. The curves agree well with experimental points in all cases over the entire field strength region.

By using a weight-average degree of polymerization of 943, the permanent dipole moment per residue was calculated to be 2.2—2.4 D (1 D=3.336×10^{-30} C m). Such values are about half of the known values of the polypeptide main chain residue moment (4.8—5.0 D/res).[36] In fact, previously obtained values are 5.3 D/res for PGA and 3.5—4.0 D/res for PBLG.[18,19] This may be due to the side chain conformation of PMLG, which differs from that of PGA and PBLG, that is, the side chain of PMLG may be oriented so as to cancel the main chain moment more effectively. Wada[36] has discussed some possible conformations of the side chain of polypeptides and the values of dipole moments associated with these conformations. He pointed out that a side chain moment of about 2.5 D/res, at maximum, may direct in opposition to the permanent dipole moment of the main chain. Thus, the small value of the permanent dipole moment of PMLG in HF2P, as revealed in the present work, can be explained by the side chain conformation.

Decay Process of PMLG. The decay portion of a RPEB signal is related to the rotational relaxation time of a solute molecule. From the decay curve, the electric birefringence-average relaxation time, $\langle\tau\rangle_{EB}$, may be obtained by the area method.[37] Figure 6 shows plots of $\langle\tau\rangle_{EB}$ for PMLG solutions at four concentrations against the square of the steady-state field strength applied prior to the decay. A slight dependence of $\langle\tau\rangle_{EB}$ on concentration was observed, probably because of the solute-solute interaction of PMLG molecules. Values of $\langle\tau\rangle_{EB}$ also depend on field strength, indicating that this PMLG sample is polydisperse

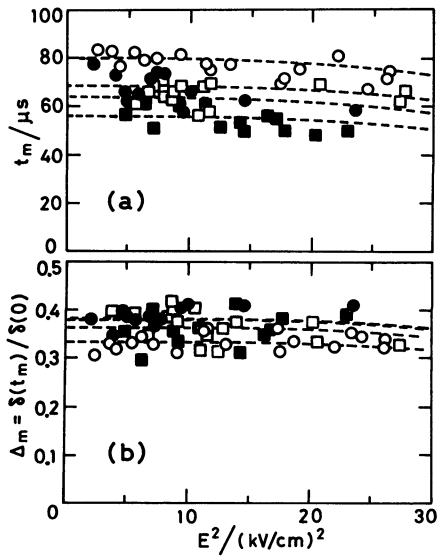

Fig. 5. The field strength dependence of the minimum position in the reverse-transient signal of PMLG in HF2P. (a) The time required for the signal to reach the minimum, t_m, and (b) the normalized phase retardation at t_m, $\Delta_m=\delta(t_m)/\delta(0)$. Symbols are the same as in Fig. 2. The limiting values of $(t_m)_{E\to 0}$ and $(\Delta_m)_{E\to 0}$ are given in Table 1.

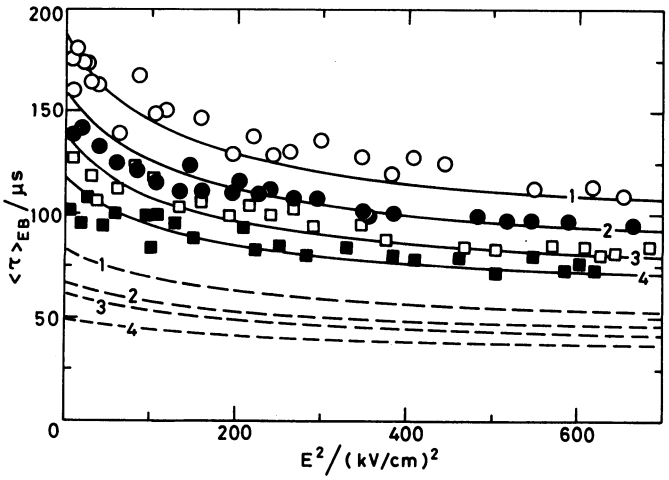

Fig. 6. The electric birefringence-average relaxation time, $\langle\tau\rangle_{EB}$, versus the square of the field strength before the start of decay. Symbols are the same as in Fig. 2. The solid lines were calculated with the decay parameters, while the dashed lines were calculated with the reverse-transient parameters. Numerals indicate the concentrations: (1) 7.82 mM, (2) 3.52 mM, (3) 1.41 mM, and (4) 0.49 mM.

TABLE 2. ELECTROOPTICAL AND HYDRODYNAMIC PROPERTIES OF PMLG IN HF2P, OBTAINED FROM THE ANALYSIS OF THE REVERSE PORTIONS OF RPEB SIGNALS

c / mM	l_w / Å	l_w/l_n	$(\beta_w)^2/2\gamma_w$	μ_w / 10^3D[a]	$\Delta\alpha_w$ / 10^{-17}cm^3[b]	$(g_3-g_1)\times10^3$
7.82	1300	1.12	2.9	2.25	4.2	2.6
3.52	1260	1.10	2.0	2.12	5.5	2.4
1.41	1230	1.10	2.0	2.06	5.1	2.7
0.49	1190	1.08	2.0	2.06	5.1	2.6

a) 1D=3.336×10^{-30} C m. b) 1 cm^3=1.113×10^{-16} F m^2

with respect to molecular length.[17]

The field strength dependence of $\langle\tau\rangle_{EB}$ can be expressed by the following equation, which takes into account the molecular length distribution:[17]

$$\langle\tau\rangle_{EB} = \frac{\int_a^b \tau(l)\Phi(\beta(l), \gamma(l))lf_n(l)dl}{\int_a^b \Phi(\beta(l), \gamma(l))lf_n(l)dl}. \quad (8)$$

With the aid of Eq. 8, the parameters (l_w, l_w/l_n) can be obtained from decay signals quite independently without relying on the result of the reverse-transient signals given in the preceding section. At infinitely high fields, Φ approaches unity, and the $\langle\tau\rangle_{EB}$ becomes the weight-average relaxation time $\langle\tau\rangle_w$,[17] which does not depend on the electric parameters $\beta(l)$ and $\gamma(l)$, but only on the parameters (l_w, l_w/l_n). The theoretical relationships between $\langle\tau\rangle_w$ and the parameters (l_w, l_w/l_n) were calculated from Eq. 4 in Ref. 17. The results are shown in Fig. 7, where the dashed lines are experimental values of $\langle\tau\rangle_w$. These were obtained by extrapolating observed values of $\langle\tau\rangle_{EB}$,

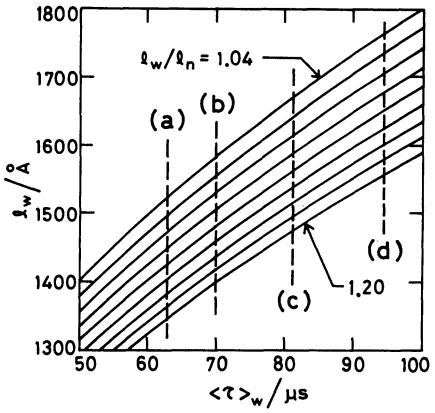

Fig. 7. Theoretical relationship between the weight-average relaxation time, $\langle\tau\rangle_w$, and the weight-average length, l_w, with the degree of polydispersity, l_w/l_n, as parameter. Values of l_w/l_n range between 1.04 and 1.20 at intervals of 0.02. The logarithmic-normal distribution was used. The relaxation time $\tau(l)$ was calculated by using Broersma's equation with a diameter 2b of 10.5 Å. Dashed lines indicate the experimental values of $\langle\tau\rangle_w$, for concentrations of (a) 0.49 mM, (b) 1.41 mM, (c) 3.52 mM, and (d) 7.82 mM.

which were plotted either against E^{-1} or against E^{-2}, to infinitely high field strength.[17] Several sets of paired values (l_w, l_w/l_n) can be obtained from the intersections between the theoretical curves and each dashed line. With each pair (l_w, l_w/l_n) thus evaluated, the theoretical curves of Δn *vs.* E^2 and of $\langle\tau\rangle_{EB}$ *vs.* E^2 can be computed from Eqs. 1 and 8 at various values of [$(\beta_w)^2/2\gamma_w$, β_w] as parameters. By matching these theoretical curves with experimentally observed plots of δ *vs.* E^2 (Fig. 2) and of $\langle\tau\rangle_{EB}$ *vs.* E^2 (Fig. 6), the best set of values can be searched for [l_w, l_w/l_n, $(\beta_w)^2/2\gamma_w$, β_w] by the trial-and-error method (this procedure is referred to as "procedure I"), and then μ_w, $\Delta\alpha_w$, and (g_3-g_1) may be separately evaluated. These values are all given in Table 3. The solid curves in Fig. 6 represent the theoretical $\langle\tau\rangle_{EB}$ *vs.* E^2 curves, which were calculated from Eq. 8. They are all in good agreement with experimental values, thus indicating that the parameters [l_w, l_w/l_n, $(\beta_w)^2/2\gamma_w$, β_w] were evaluated correctly.

Similarly to the above, the $\langle\tau\rangle_{EB}$ *vs.* E^2 curves can also be calculated by using the parameters obtained from the reverse-transient signals (Table 2). These theoretical curves are shown in Fig. 6 by dashed curves, but surprisingly they differ from the observed points of $\langle\tau\rangle_{EB}$ far beyond experimental errors. This unexpected result indicates that the reverse process for an RPEB signal is different from the decay. Some possible explanations will be considered in the following sections.

Simulation of RPEB Signal. With the two sets of parameters [l_w, l_w/l_n, $(\beta_w)^2/2\gamma_w$], one from the reverse-transient process and the other from the decay process, the theoretical curves of the rise, reverse, and decay portions of RPEB signals of PMLG at various concentrations were calculated from Eqs. 2, 4, and 5, in order to justify the correctness of the estimated parameters. The RPEB signal at 3.52 mM was calculated as an example and is shown in Fig. 8. The rise (Fig. 8(a)) and reverse (Fig. 8(b)) portions of the observed data (dots) under an applied external field are well reproduced by the curve (solid line) calculated with the reverse-transient parameters [l_w=1260 Å, l_w/l_n=1.10, $(\beta_w)^2/2\gamma_w$=2.0], but definitely deviate from the curve (dash-dot line) calculated with the decay parameters [l_w=1530 Å, l_w/l_n=1.15, $(\beta_w)^2/2\gamma_w$=3.0]. On the other hand, the observed decay data (Fig. 8(c)) transfer, upon removal of the pulse field, from the theoretical curve with the reverse-transient parameters

Table 3. Electrooptical and hydrodynamic properties of PMLG in HF2P, obtained from the analysis of the decay portions of RPEB signals

c / mM	l_w[a] / Å	l_w/l_n	$(\beta_w)^2/2\gamma_w$	μ_w / 10^3D	$\Delta\alpha_w$ / 10^{-17}cm^3	$(g_3-g_1)\times10^3$
7.82	1610	1.15	3.0	2.23	3.7	2.7
	1650	(1.12)[b]				
3.52	1530	1.15	3.0	2.14	3.7	2.8
	1590	(1.10)[b]				
1.41	1450	1.15	3.0	2.18	3.9	2.8
	1510	(1.10)[b]				
0.49	1410	1.14	3.0	2.18	3.9	2.8
	1470	(1.08)[b]				

a) The lengths l_w in the upper row were obtained by "procedure I" and those in the lower row by "procedure II". b) Values in parentheses are obtained from the reverse-transient portions (Table 2).

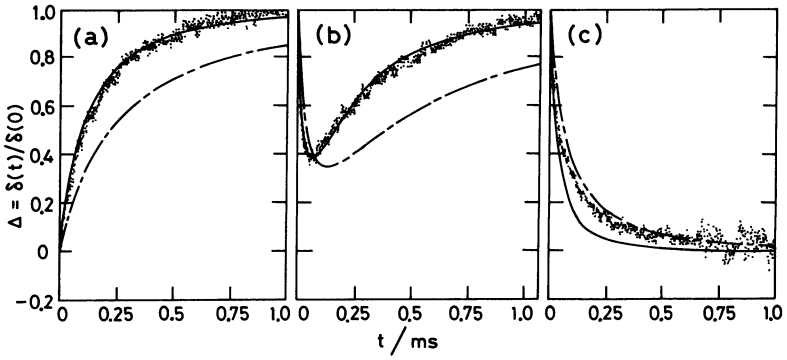

Fig. 8. Comparison of the rise (a), reverse (b), and decay (c) portions of a normalized RPEB signal of PMLG at 3.52 mM with theoretical curves. The observed data were average of 150 signals taken below 3.5 kV/cm in the Kerr law region. The solid curves represent the simulated RPEB signal which was calculated with the reverse-transient parameters (l_w=1260 Å, l_w/l_n=1.10, $(\beta_w)^2/2\gamma_w$= 2.0), while the dash-dot-dashed curves represent the signal calculated with the decay parameters (l_w=1530 Å, l_w/l_n=1.15, $(\beta_w)^2/2\gamma_w$=3.0). The logarithmic-normal distribution (2b=10.5 Å) was assumed.

to the one with the decay parameters in the time course between 20—200 μs. The same results have been obtained for many RPEB signals at other concentrations and field strengths. Any RPEB signal of PMLG in HF2P must therefore contain two processes with different sets of molecular parameters during the application and removal of an external electric field.

Since the steady-state and the reverse-transient are observed under the presence of an electric field, a combination of these data should give consistent results. On the other hand, the decay parameters obtained with the steady-state data by "procedure I" should only be apparent. It is now clear, therefore, that the decay portion of the RPEB signal must be analyzed without recourse to the steady-state value. By assuming that the PMLG molecules change identically regardless of their lengths under an electric field, the degree of polydispersity l_w/l_n may be considered to be constant in the presence and absence of the field. Then, with the value of l_w/l_n in Table 2, which was obtained from the reverse portion, the weight-average molecular length l_w can be determined from $<\tau>_w$ (this is referred to as "procedure II"), as was shown in Fig. 7. The values of l_w thus obtained are given in the second row at each concentration in Table 3. The difference in l_w estimated from two procedures (I and II) is no more than 60 Å or 4%, being comparable with experimental errors. Therefore, the difference in the molecular lengths obtained from the reverse (Table 2) and the decay (Table 3) should be attributed to the direct effect of an applied electric field and not to the analytical procedures.

The reverse-transient portion is a process under the influence of an applied field (Fig. 8(b)): an observed value of t_m at the minimum position is 69 μs, while the one calculated with the reverse-transient parameters is also 69 μs, clearly differing from the one calculated with the decay parameters, 136 μs. It has been shown that t_m does not depend on the electric properties, such as $(\beta_w)^2/2\gamma_w$ and μ_w, but depends only on l_w and l_w/l_n, even if a sample is polydisperse.[18] Therefore, the discrepancy resulting from the application and removal of a pulse field can clearly be attributed to the difference in molecular lengths of PMLG helices. Four possible explanations for this discrepancy may be considered. (1) The PMLG helices are flexible enough to be bent under an electric field. (2) They associate to form molecular aggregates in HF2P which transform from one type to another, when the electric pulse is applied. (3) In HF2P they are partly broken to have, *e.g.*, a coiled tail by the electric field. (4) They are subjected to field-induced conformational transition.

In the case of (1), the slightly bending PMLG helices in solution may be stretched under an electric field. The RPEB signal would rise fast at the initial stage, then slow down due to a rotational relaxation of straightened longer molecules. This idea is not supported by the experimental signals in the rise portion. Conversely, the originally straight PMLG helices may be bent momentarily due to an abrupt rotation caused by the applied field. Here, they must return to the original form, when the RPEB signal reaches the steady-state. They should then behave like a straight rod in the subsequent decay process, but the actual decay curve contains a transfer (Fig. 8(c)). Moreover, we have studied the RPEB of a PBLG sample with an average molecular length of 2450 Å.[19,29] This PBLG helix may be fairly flexible, considering the persistence length of PBLG (about 1200 Å);[38,39] yet the $<\tau>_{EB}$ *vs.* E^2 curve was well reproduced by the parameters which were obtained from the reverse portion. The difference between reverse-transient and decay processes can not be attributed to the flexibility of PMLG molecules.

The second case (2) may be ruled out immediately because intermolecular association does not occur in this solution, as shown in Fig. 4. This notion is additionally supported by the degree of polymerization obtained from the intrinsic viscosity in DCA (DP= 943). If the conformation of PMLG is the α-helix,[40,41] the length should be about 1400 Å (1.5 Å×943), which agrees well with the value of l_w, as obtained from the analysis of the decay portion of RPEB signals (Table 3).

Therefore, the PMLG helices undoubtedly remain molecularly dispersed at low concentration. The third case (3) may be excluded on the basis that, if a PMLG helix is partially broken by the electric field, the helix should be steadily unwound with an increase in field strengths. In such a case, the field strength dependence of the steady-state value could no longer be simulated by a single set of parameters [l_w, l_w/l_n, $(\beta_w)^2/2\gamma_w$, β_w] in Table 2, which would change continuously and considerably by the destruction of helices with increasing field strength. Figure 2 shows clearly that this is contrary to the experimental results. The last case (4) remains as the most probable and more precise discussions will be given in the following sections.

Intrinsic Viscosity and Molecular Conformation. Once taken under the same conditions, both the intrinsic viscosity and the RPEB data in HF2P may be combined to obtain the hydrodynamical diameter of a PMLG molecule in the following way.[29] Since the intrinsic viscosity was determined in the absence of electric field, the parameters (l_w, l_w/l_n) evaluated from the decay signal must be used. These values were first calculated for three diameters (10, 10.5, and 11 Å) by "procedure II"; hence, three sets of (l_w, l_w/l_n). Three intrinsic viscosity values, $<[\eta]>$, at each concentration were calculated with the aid of Eq. 6 for the three parameter sets. The results are shown with open symbols in Fig. 9(a). A value of 0.763 was used for the partial specific volume of PMLG.[7,8] By comparing the values of $<[\eta]>$ extrapolated to zero concentration with the observed value of $[\eta]_{HF2P}$, a diameter of 10.5 Å was selected for $2b$. For comparison, the values of $<[\eta]>$ were also calculated by using the parameters (l_w, l_w/l_n) evaluated from the decay signal by "procedure I," and are plotted with closed symbols in Fig. 9(a). The result clearly indicates that the diameter is not affected by two analytical methods, and that the value of 10.5 Å is adequate for the diameter of a PMLG helix. It must be stated that, for all analyses in the preceding sections, the value of 10.5 Å was used as the best hydrodynamic diameter of PMLG.

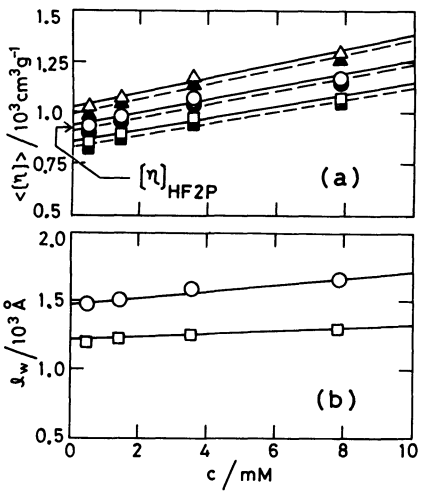

Fig. 9. (a) The dependence of the calculated intrinsic viscosities, $<[\eta]>$, and (b) the dependence of the length l_w on concentration of PMLG in HF2P. The diameters are 2b=10 Å (△, ▲), 10.5 Å (○, ●), and 11 Å (□, ■). The theoretical values were calculated from the parameters of "procedure I" (open symbols and solid lines), and of "procedure II" (closed symbols and dashed lines). Arrow indicates the observed $[\eta]_{HF2P}$. The values of l_w (○) were obtained from the decay portion (lower rows in Table 3) and (□) from the reverse portion (Table 2).

Molecular Length of PMLG. Figure 9(b) shows two plots of the weight-average molecular length l_w against concentration; one from the reverse-transient (squares) and the other from the decay (circles). Being dependent on concentration, probably due to solute-solute interaction, values of l_w should be extrapolated to zero concentration, in order to obtain the molecular length free from such interaction. The limiting values are: $(l_w)_{R,c\to0}$=1210 Å from the reverse-transient process and $(l_w)_{D,c\to0}$=1470 Å from the decay process. Thus, the length of PMLG helix is shorter by about 18% under an electric field than that in the absence of the field. From the degree of polymerization of this PMLG sample, the length per residue is determined to be 1.56 Å/res from $(l_w)_{D,c\to0}$ and is 1.29 Å/res from $(l_w)_{R,c\to0}$. It should be pointed out that these values nearly correspond to the α-helix (1.5 Å/res)[40,41] and the ω-helix (1.3 Å/res),[42-44] respectively.

A Possible Model of Conformational Transition. Finally, a plausible mechanism of the conformational transition induced by the electric field will be discussed on the basis of reversible helix-to-helix alteration. A helical segment is illustrated on the left-hand side in Fig. 10, where an α-helix structure is used as a model. A peptide residue of the main chain is inclined at 64.5° relative to the helix axis, and the length per residue, $h_D \equiv (l_w)_{D,c\to0}/DP_w$, is taken to be 1.56 Å. The plane of the peptide unit is assumed to be parallel to the axis. Although the direction of the permanent dipole moment has not been fully established as yet, it is generally assumed to make an angle of 56.2° relative to the

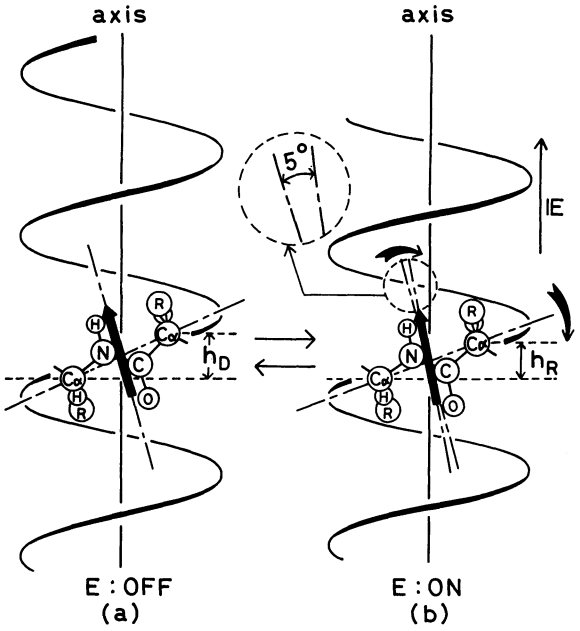

Fig. 10. A possible mechanism for electric field-induced conformational transition of PMLG in HF2P. (a) Electric field is off, and (b) electric field is on. See text for details.

C–N bond.[36,45] A probable direction is indicated with an arrow.

When an electric pulse field is applied, the dipole moment in each peptide group would be oriented toward the helix axis because of the interaction between the field strength and the dipole moment. As a result, the axial translation per residue may be shortened, as shown on the right-hand side of Fig. 10. The PMLG helix would be distorted in such a way that a shorter helix appears. In order to lower the axial translation by about 18% ($h_R \equiv (l_w)_{R,c\to 0}/DP_w = 1.29$ Å), the direction of the permanent dipole moment would have to be rotated clockwise around the normal to the helix axis by no more than 5 degrees, as indicated on the right-hand side of Fig. 10. It is reasonable to believe that this conformational transition occurs in the low field strength region (the lowest field strength in this study is about 1 kV/cm), for the change of the moment direction could possibly be less than 5° being associated with no drastic alteration of the helix backbone or hydrogen-bond breaking. The change in axial translation per residue from 1.56 Å to 1.29 Å is in the same order as that of the α- to ω-helices. Both helices belong to the same intramolecular hydrogen-bond-forming class and their stability is energetically comparable.[43,46] The PMLG helix in HF2P probably transforms from an α-helix to an ω-helix in the presence of an electric field. Matsumoto *et al.*[47] measured the electric birefringence of poly(α-L-glutamic acid) in a dimethyl sulfoxide–methanol mixtures. They discussed the possibility that the PGA helix (presumably the α-helix) is induced to be the ω-helix by solvent composition.

In the present work, the electric field-induced conformational transition of PMLG in HF2P was discovered in the course of an extensive analysis of RPEB signals. The usefulness of the RPEB method is evident in investigating the molecular properties of polypeptides in solutions subjected to electric fields.

Conclusion

By analyzing the reverse and decay portions of the RPEB signal of PMLG independently, two sets of the same molecular parameters (l_w, l_w/l_n, μ_w, $\Delta\alpha_w$) were obtained. The length l_w from the reverse portion differs from the decay portion, the former being shorter about 18% than the latter. The dipole moment per residue of PMLG (2.2—2.4D) is only about one half that of PGA or PBLG.[18,19] The side chain moment of PMLG must considerably cancel the contribution from the main chain moment. A plausible mechanism was proposed to explain the reversible shortening of the helical length upon application of an external electric field. With due considerations of the parameters evaluated in this work, it was concluded that the PMLG molecule probably forms an α-helix in the absence of an electric field, but transforms to another helix, possibly an ω-helix, by the electric field.

The author wishes to thank Associate Professor Kiwamu Yamaoka for his continuous support and encouragement in the course of this study. The author also wishes to thank Mr. Shinobu Yamamoto for his skilled assistance in computer programming.

References

1) W. B. Gratzer, G. M. Holzwarth, and P. Doty, *Proc. Natl. Acad. Sci. USA*, **47**, 1785 (1961).
2) G. Holzwarth and P. Doty, *J. Am. Chem. Soc.*, **87**, 218 (1965).
3) R. Mandel and G. Holzwarth, *J. Chem. Phys.*, **57**, 3469 (1972).
4) W. Moffitt, *Proc. Natl. Acad. Sci. USA*, **42**, 736 (1956).
5) W. Moffitt, *J. Chem. Phys.*, **25**, 467 (1956).
6) W. Moffitt, D. D. Fitts, and J. G. Kirkwood, *Proc. Natl. Acad. Sci. USA*, **43**, 723 (1957).
7) Y. Okamoto and R. Sakamoto, *Nippon Kagaku Zasshi*, **90**, 669 (1969).
8) Y. Ishimuro, S. Yamaguchi, F. Hamada, and A. Nakajima, *Biopolymers*, **20**, 2499 (1981).
9) "Molecular Electro-Optics, Part 2," ed by C. T. O'Konski, Marcel Dekker, New York (1978).
10) K. Yoshioka and H. Watanabe, "Pyhsical Principles and Techniques of Protein Chemistry, Part A," ed by S. J. Leach, Academic Press, New York (1969), Chap. 7.
11) K. Yamaoka, Ph. D. Dissertation, University of California, Berkeley, CA, 1964.
12) M. Matsumoto, H. Watanabe, and K. Yoshioka, *Biopolymers*, **6**, 929 (1968).
13) S. Kobayasi, *Biopolymers*, **6**, 1491 (1968).
14) M. Matsumoto, H. Watanabe, and K. Yoshioka, *Kolloid Z. Z. Polym.*, **250**, 298 (1972).
15) M. Matsumoto, H. Watanabe, and K. Yoshioka, *Biopolymers*, **9**, 1307 (1970).
16) J. Schweitzer and B. R. Jennings, *Biopolymers*, **11**, 1077 (1972).
17) K. Yamaoka and K. Fukudome, *Bull. Chem. Soc. Jpn.*, **56**, 60 (1983).
18) K. Yamaoka and K. Ueda, *J. Phys. Chem.*, **86**, 406 (1982).
19) K. Ueda, M. Mimura, and K. Yamaoka, *Biopolymers*, in press.
20) H. Watanabe, *Nippon Kagaku Zasshi*, **85**, 603 (1964).
21) K. Yamaoka, T. Ichibakase, K. Ueda, and K. Matsuda, *J. Am. Chem. Soc.*, **102**, 5109 (1980).
22) K. Yamaoka, S. Yamamoto, and K. Ueda, *Polymer Preprints, Japan*, **32**, 689 (1983).
23) K. Yamaoka and E. Charney, *Macromolecules*, **6**, 66 (1973).
24) C. T. O'Konski, K. Yoshioka, and W. H. Orttung, *J. Phys. Chem.*, **63**, 1558 (1959).
25) I. Tinoco, Jr. and K. Yamaoka, *J. Phys. Chem.*, **63**, 423 (1959).
26) S. Broersma, *J. Chem. Phys.*, **32**, 1626 (1960).
27) The type of distribution function is not too critical when a well fractionated sample is utilized. See also Ref. 19.
28) W. D. Lansing and E. O. Kraemer, *J. Am. Chem. Soc.*, **57**, 1369 (1935).
29) K. Ueda, M. Nomura, and K. Yamaoka, *Biopolymers*, **22**, 2077 (1983).
30) H. L. Frisch and R. Simha, "Rheology, Vol. 1," ed by F. R. Eirich, Academic Press, New York (1956), Chap. 14.
31) C. Wolff, A. Silberberg, Z. Priel, and M. N. Layec-Raphalen, *Polymer*, **20**, 281 (1979).
32) H. Watanabe, *Nippon Kagaku Zasshi*, **86**, 179 (1965).
33) J. C. Powers, Jr. and W. L. Peticolas, *Biopolymers*, **9**, 195 (1970).
34) W. Pyżuk and T. Krupkowski, *Makromol. Chem.*, **178**, 817 (1977).
35) K. Yamaoka and K. Matsuda, *Macromolecules*, **14**, 595 (1981).

36) A. Wada, *Adv. Biophys.*, **9**, 1 (1976).
37) K. Yoshioka and H. Watanabe, *Nippon Kagaku Zasshi*, **84**, 626 (1963).
38) V. N. Tsvetkov, I. N. Shtennikova, V. S. Skazka, and E. I. Rjumtsev, *J. Polym. Sci., Part C*, **16**, 3205 (1968).
39) S. Itou, N. Nishioka, T. Norisuye, and A. Teramoto, *Macromolecules*, **14**, 904 (1981).
40) L. Pauling, R. B. Corey, and H. R. Branson, *Proc. Natl. Acad. Sci. USA*, **37**, 205 (1951).
41) L. Pauling and R. B. Corey, *Proc. Natl. Acad. Sci. USA*, **37**, 235 (1951).
42) W. L. Bragg, J. C. Kendrew, and M. F. Perutz, *Proc. Roy. Soc.*, **A203**, 321 (1950).
43) E. M. Bradbury, L. Brown, A. R. Downie, A. Elliott, W. E. Hanby, and T. R. R. McDonald, *Nature*, **183**, 1736 (1959).
44) E. M. Bradbury, L. Brown, A. R. Downie, A. Elliott, R. D. B. Fraser, and W. E. Hanby, *J. Mol. Biol.*, **5**, 230 (1962).
45) D. A. Brant, W. G. Miller, and P. J. Flory, *J. Mol. Biol.*, **23**, 47 (1967).
46) R. E. Dickerson and I. Geis, "The Structure and Action of Proteins," Harper and Row, New York (1969), Chap. 2.
47) M. Matsumoto, H. Watanabe, and K. Yoshioka, *Biopolymers*, **12**, 1729 (1973).